1538

Proc. Indian Acad. Sci. (Earth Planet. Sci.), Vol. 101, No. 2, June 1992, pp. 109–122.

An efficient optimum interpolation scheme for objective analysis over Indian region

S K SINHA, S G NARKHEDKAR and S RAJAMANI
Indian Institute of Tropical Meteorology, Pashan Road, Pune 411 008, India

MS received 17 December 1991; revised 5 May 1992

Abstract. In the optimum interpolation scheme, the weights for the observations are computed by solving a set of linear equations for every grid point. As the number of observations increases particularly over data-rich regions, the matrix dimension increases and the computer time required to solve these equations to determine weights increases considerably. In order to reduce the computer time for computing the weights, Tanguay and Robert suggested schemes in which the gaussian function representing the autocorrelation function has been approximated by a second-order and also by a fourth-order Taylor series expansion. This resulted in the solution of matrices of order 4 or 9 respectively to obtain weighting functions irrespective of the number of observations used in the analysis. In the present study, the analyses of mean sea level pressure and geopotential height at 700 mbar level have been carried out for five days using the above two schemes and the regular OI scheme. The analyses are found to be similar in all the three cases suggesting that a lot of computer time could be saved without sacrificing the analysis accuracy by using the modified scheme in which the second-order approximation is utilized.

Keywords. Efficient optimum interpolation; weighting function; autocorrelation function; structure function; objective analysis.

1. Introduction

Gandin (1963) introduced the objective analysis technique of optimum interpolation (OI) in meteorology. He derived an expression for the weighting functions for the observing stations with respect to the grid points incorporating the physical characteristics of the variable over the domain. This method is now widely used in assimilation procedures for large scale prediction models (McPherson *et al* 1979; Lorenc 1981; Hollingsworth *et al* 1985). However, this OI scheme is computationally expensive since the time taken to determine weights from the linear system of equations strongly depends on the number of observations selected. Bratseth (1986) proposed a successive correction scheme that converges towards a statistical interpolation scheme in the limit and is economical. Seaman (1988) and Franke (1988) further discussed this approach.

In this paper, we describe two other optimum interpolation schemes suggested by Tanguay and Robert (1990) in which the autocorrelation function is approximated by a parabolic (second-order approximation of Taylor series) and a fourth-order polynomial (FOP) respectively and the weights are obtained by solving 4×4 matrix and 9×9 matrix irrespective of the number of observations. While these schemes save computer time, whether they will also result in accurate analysis is the objective of this study. The geopotential height at 700 mbar and MSL pressure was analysed

with the univariate optimum interpolation scheme (Gaussian) as well as with the two new schemes (parabolic and FOP) and were studied.

2. Methodology

2.1 *Basic equations of optimum interpolation scheme*

Let f_i, $\hat{f}_i$, $\tilde{f}_i$ and $\hat{f}'_i$ be the true value, observed value, the initial guess value and the anomaly which is the deviation of the observed value from the initial guess value at the station i, then we have the following relations

$$\hat{f}'_i = \hat{f}_i - \tilde{f}_i,$$
$$\hat{f}_i = f_i + \varepsilon_i, \tag{1}$$

where ε_i is the total error in the observed value. The analysed value or the interpolated value, f_o, at the grid point o, is given by

$$f_o = \tilde{f}_o + f'_o,$$

where the anomaly f'_o is given as a linear combination of weighted anomalies at the stations surrounding the grid points:

$$\text{i.e.} \quad f'_o = \sum_{i=1}^{n} \hat{f}'_i W_i + I_o, \tag{2}$$

where W_i is the weight and I_o the error in the interpolation.

In OI schemes, the weights are determined such that the quantity E is minimum.

$$E = \overline{I_o^2} = \overline{\left[f'_o - \sum_{i=1}^{n} (f'_i + \varepsilon_i) W_i \right]^2}, \tag{3}$$

where the bar represents an average over a large number of grid points. This is achieved by making

$$\partial E / \partial W_i = 0. \tag{4}$$

We make two important assumptions. First, the total error ε_i is independent of the anomaly of the true value,

$$\text{i.e.} \quad \overline{\varepsilon_i f'_i} = 0, \tag{5}$$

and also independent of the total error, ε_j at other station, j.

$$\text{i.e.} \quad \overline{\varepsilon_i \varepsilon_j} = \begin{cases} 0, \text{ when } i \neq j \\ \sigma_{\varepsilon_i}^2, \text{ when } i = j. \end{cases} \tag{6}$$

Secondly, the variances are assumed to be homogeneous and covariances are both homogeneous and isotropic. Isotropic condition implies that the correlation coefficient depends only on the distance between two locations and not on their orientations.

With these assumptions, (3) yields n equations with n unknowns ω_i $(i = 1, 2, \ldots n)$.

$$\text{i.e.} \quad \sum_{i=1}^{n} [\mu(\rho_{ij}) + \hat{\lambda}\delta_{ij}]\omega_i = \mu(\rho_{oj}), \; j = 1, \ldots n, \tag{7}$$

where ρ_{ij} refers to the distance between two locations (x_i, y_i) and (x_j, y_j).

$$\mu(\rho_{ij}) = \overline{\hat{f}'_i \hat{f}'_j}/\sigma_o^2, \; \mu(\rho_{oj}) = \overline{\hat{f}'_j f'_o}/\sigma_o^2, \; \hat{\lambda} = \sigma_{\varepsilon_j}^2/\sigma_o^2,$$

$\mu(\rho_{ij})$ is the autocorrelation for a pair of stations i and j, and $\mu(\rho_{oj})$ the autocorrelation between grid point o and the station j. $\sigma_{\varepsilon_j}^2$ is random error and σ_o^2 the corrected average variance for the region.

The random error $\sigma_{\varepsilon_j}^2$ required for calculation of $\hat{\lambda}$ is obtained from structure function. The true structure function

$$\beta(\rho_{ij}) = \overline{(f'_i - f'_j)^2}$$

and the estimated structure function

$$\hat{\beta}(\rho_{ij}) = \overline{(\hat{f}'_i - \hat{f}'_j)^2}$$

are related through the following relation:

$$\hat{\beta}(\rho_{ij}) = \beta(\rho_{ij}) + 2\sigma_{\varepsilon_j}^2$$

$\beta(\rho_{ij})$ becomes zero when ρ_{ij} becomes zero but $\hat{\beta}(\rho_{ij})$ need not become zero at the same location. So when ρ_{ij} becomes zero,

$$\hat{\beta}(0) = 2\sigma_{\varepsilon_j}^2.$$

In other words, $2\sigma_{\varepsilon_j}^2$ is estimated by fitting a curve to the computed structure function, β plotted against distance, ρ_{ij}, and extrapolating the curve until it intersects the axis of $\hat{\beta}(\rho_{ij})$ at $\rho_{ij} = 0$. The autocorrelation function curve tends towards zero at ρ_{ij} goes to infinity. Several autocorrelation functions (candidate correlation function) have been used by many researchers (Julian and Thiebaux 1975; Thiebaux 1975; Seaman and Hutchinson 1985; Shaw *et al* 1987) to model the observed autocorrelations. In this experiment we have chosen the following gaussian function to model the observed autocorrelations

$$\mu(\rho_{ij}) = (1 - \hat{\lambda}) \exp(-\rho_{ij}^2/S^2). \tag{8}$$

The number of arithmetic operations required to invert the autocorrelation matrix of order n goes roughly n^3, hence the computational cost for solving the system of equation (7) is high when the number of observations increases. Therefore, most operational optimum interpolation schemes restrict the number of observation to a certain limit.

2.2 *Basic equations for efficient OI*

In this efficient OI scheme the autocorrelation function $\mu(\rho_{ij})$ is approximated by a parabola. This is done by expanding the gaussian function $(1 - \hat{\lambda}) \exp(-\rho_{ij}^2/S^2)$ in

Taylor series and considering the first three terms, we have

$$\mu(\rho_{ij}) = (1 - \hat{\lambda})[1 - (\rho_{ij}/S)^2], \tag{9}$$

where

$$\rho_{ij} = [(x_i - x_j)^2 + (y_i - y_j)^2]^{1/2}. \tag{10}$$

Now resolving analytically the system of equation (7) with the above parabolic autocorrelation functions we get

$$\lambda\omega_j + \sum_{i=1}^{n} [1 - (X_i - X_j)^2 - (Y_i - Y_j)^2]\omega_i = [1 - X_j^2 - Y_j^2], j = 1, \ldots n, \tag{11}$$

where

$$\lambda = \hat{\lambda}/(1 - \hat{\lambda}),\ X_i = (x_i - x_o)/S \text{ and } Y_i = (y_i - y_o)/S.$$

Equation (11) can be further written as

$$\lambda\omega_j = \left[1 - \sum_{i=1}^{n} \omega_i + \sum_{i=1}^{n} \omega_i(X_i^2 + Y_i^2)\right] - 2X_j \sum_{i=1}^{n} \omega_i X_i$$
$$- 2Y_j \sum_{i=1}^{n} \omega_i Y_i - (X_j^2 + Y_j^2)\left(1 - \sum_{i=1}^{n} \omega_i\right), j = 1, \ldots n. \tag{12}$$

The summations $\Sigma_{i=1}^{n}$ in (12) can be considered as constants since they do not depend on j. Thus (12) can be written as

$$\omega_j = A + BX_j + CY_j + D(X_j^2 + Y_j^2), j = 1, \ldots n, \tag{13}$$

where

$$A = \frac{1}{\lambda}\left[1 - \sum_{i=1}^{n} \omega_i + \sum_{i=1}^{n} \omega_i(X_i^2 + Y_i^2)\right],$$

$$B = -\frac{2}{\lambda} \sum_{i=1}^{n} \omega_i X_i,$$

$$C = -\frac{2}{\lambda} \sum_{i=1}^{n} \omega_i Y_i,$$

$$D = -\frac{1}{\lambda}\left(1 - \sum_{i=1}^{n} \omega_i\right) \tag{14}$$

Let us define

$$S_{kl} = \sum_{i=1}^{n} X_i^k Y_i^l. \tag{15}$$

Replacing j by i in (13), we have

$$\omega_i = A + BX_i + CY_i + D(X_i^2 + Y_i^2), i = 1, \ldots n. \tag{16}$$

With the help of (15), we can write the above equation as

$$\sum_{i=1}^{n} \omega_i = AS_{00} + BS_{10} + CS_{01} + D(S_{20} + S_{02}).$$

Similarly

$$\sum_{i=1}^{n} \omega_i X_i = AS_{10} + BS_{20} + CS_{11} + D(S_{30} + S_{12}),$$

$$\sum_{i=1}^{n} \omega_i Y_i = AS_{01} + BS_{11} + CS_{02} + D(S_{21} + S_{03})$$

$$\sum_{i=1}^{n} \omega_i (X_i^2 + Y_i^2) = A(S_{20} + S_{02}) + B(S_{30} + S_{12}) + C(S_{21} + S_{03}) + D(S_{40} + 2S_{22} + S_{04}). \tag{17}$$

Equation (14) can be rewritten as

$$-\lambda(A + D) + \sum_{i=1}^{n} \omega_i (X_i^2 + Y_i^2) = 0,$$

$$\frac{\lambda}{2} B + \sum_{i=1}^{n} \omega_i X_i = 0,$$

$$\frac{\lambda}{2} C + \sum_{i=1}^{n} \omega_i Y_i = 0,$$

$$-\lambda D + \sum_{i=1}^{n} \omega_i = 1. \tag{18}$$

Replacing the summations $\Sigma_{i=1}^{n}$ in (18) by their associated expression (17), we get

$$-\lambda(A + D) + A(S_{20} + S_{02}) + B(S_{30} + S_{12}) + C(S_{21} + S_{03}) + D(S_{40} + 2S_{22} + S_{04}) = 0$$

$$\frac{\lambda}{2} B + AS_{10} + BS_{20} + CS_{11} + D(S_{30} + S_{12}) = 0$$

$$\frac{\lambda}{2} C + AS_{01} + BS_{11} + CS_{02} + D(S_{21} + S_{03}) = 0$$

$$-\lambda D + AS_{00} + BS_{10} + CS_{01} + D(S_{20} + S_{02}) = 1. \tag{19}$$

After arranging the terms in the above system of equations and interchanging the first and the fourth rows, we have

$$\begin{bmatrix} S_{00} & S_{10} & S_{01} & S_{20} + S_{02} - \lambda \\ S_{10} & S_{20} + \frac{1}{2}\lambda & S_{11} & S_{30} + S_{12} \\ S_{01} & S_{11} & S_{02} + \frac{1}{2}\lambda & S_{21} + S_{03} \\ S_{20} + S_{02} - \lambda & S_{30} + S_{12} & S_{21} + S_{03} & S_{40} + 2S_{22} + S_{04} - \lambda \end{bmatrix} \begin{bmatrix} A \\ B \\ C \\ D \end{bmatrix} = \begin{bmatrix} 1 \\ 0 \\ 0 \\ 0 \end{bmatrix} \tag{20}$$

The above system is of order 4 and its computational time is independent of the number of observations selected to influence the grid point.

In the case when the autocorrelation function $\mu(\rho_{ij})$ is approximated by the

fourth-order Taylor series expansion, we have

$$\mu(\rho_{ij}) = (1 - \hat{\lambda})[1 - (\rho_{ij}/S)^2 + 0{\cdot}5(\rho_{ij}/S)^4], \tag{21}$$

and the weighting function ω_i takes the form

$$\omega_i = A + BX_i + CY_i + DX_i^2 + EX_i\,Y_i + FY_i^2 + G(X_i^3 + X_i\,Y_i^2) + H(X_i^2\,Y_i + Y_i^3) + I(X_i^4 + 2X_i^2\,Y_i^2 + Y_i^4), \tag{22}$$

where the 9 unknown constants A, B, C, D, E, F, G, H and I are determined by solving the symmetric matrix **M**

$$M_{11} \text{ to } M_{19}: S_{00}, S_{10}, S_{01}, S_{20}, S_{11}, S_{02}, S_{30} + S_{12},$$
$$S_{21} + S_{03}, S_{40} + 2S_{22} + S_{04} + 2\lambda,$$
$$M_{22} \text{ to } M_{29}: S_{20}, S_{11}, S_{30}, S_{21}, S_{12}, S_{40} + S_{22} - 0{\cdot}5\lambda,$$
$$S_{31} + S_{13}, S_{50} + 2S_{32} + S_{14},$$
$$M_{33} \text{ to } M_{39}: S_{02}, S_{21}, S_{12}, S_{03}, S_{31} + S_{13},$$
$$S_{22} + S_{04} - 0{\cdot}5\lambda, S_{41} + 2S_{23} + S_{05},$$
$$M_{44} \text{ to } M_{49}: S_{40} + 0{\cdot}375\lambda, S_{31}, S_{22} - 0{\cdot}125\lambda, S_{50} + S_{32},$$
$$S_{41} + S_{23}, S_{60} + 2S_{42} + S_{24} + 0{\cdot}5\lambda,$$
$$M_{55} \text{ to } M_{59}: S_{22} + 0{\cdot}25\lambda, S_{13}, S_{41} + S_{23}, S_{32} + S_{14}, S_{51} + 2S_{33} + S_{15},$$
$$M_{66} \text{ to } M_{69}: S_{04} + 0{\cdot}375\lambda, S_{32} + S_{14}, S_{23} + S_{05}, S_{42} + 2S_{24} + S_{06} + 0{\cdot}5\lambda,$$
$$M_{77} \text{ to } M_{79}: S_{60} + 2S_{42} + S_{24} - 0{\cdot}5\lambda, S_{51} + 2S_{33} + S_{15},$$
$$S_{70} + 3S_{52} + 3S_{34} + S_{16},$$
$$M_{88} \text{ to } M_{89}: S_{42} + 2S_{24} + S_{06} - 0{\cdot}5\lambda, S_{07} + 3S_{25} + 3S_{43} + S_{61}$$
$$M_{99}: S_{80} + 4S_{62} + 6S_{44} + 4S_{26} + S_{08} - 2\lambda$$

where M are the elements of the matrix **M**. The vector on the right hand side of the 9×9 system is $(1, 0, 0, 0, 0, 0, 0, 0, 0)$.

3. Data and computations

3.1 *Data and synoptic situation*

Surface pressure data of 0300 IST from land-based meteorological stations over India and the neighbouring region for the period (1975–1985) (July) were utilized for computing autocorrelation and structure functions. First GARP (the global atmospheric research program) global experiment (FGGE) analyses of 3 July to 8 July 1979 were utilized as the initial guess field and the radiosonde observations, special aircraft dropsonde data and the radiosonde data from research ships from Monex-79 for these days were used for analyses.

On 4 July 1979 there was a low pressure area over north east Bay of Bengal. This

low pressure area slowly concentrated into a depression by 7 July and 8 July the depression moved westward and crossed north Orissa coast. Thus we have a few interesting and changing synoptic situations which should be depicted properly by objective analysis schemes under examination.

3.2 *Computations*

Using daily radiosonde data for geopotential heights and MSL pressure, the autocorrelations of every station with respect to all other stations in the Indian region were computed for both the variables. Assuming isotropy and homogeneity of the autocorrelations, the values within 2° or 220 km were averaged to represent the mid-points and plotted. The above observed autocorrelation function has been modelled by a gaussian function and a parabolic function. For MSL pressure field they are shown in figure 1. Figure 2 illustrates the structure function curve for the MSL pressure field plotted against distance. Table 1 shows the value of noise-to-single ratio ($\hat{\lambda}$) for MSL pressure. Analyses for the period 4 to 8 July 1979 have been carried out. The domain of analysis is bounded by 41·250°E to 108·750°E and 1·875°N to 39·375°N. A grid size 1·875° was considered in this experiment. Previous day's analysis from FGGE was used as the initial guess field. We studied the two analyses (guassian scheme and parabolic scheme) to examine whether they represented the flow patterns properly and depicted the various monsoon systems well. Both the analyses were also compared with the FGGE analysis of the particular day. For quantitative evaluation, root mean square (RMS) errors were calculated by comparing the analyses from both schemes with the FGGE analyses. RMS errors were also computed by interpolating the objectively analysed field back to observation locations and by comparing with those observations. Similarly, objective analyses of geopotential height of 700 mbar using both the schemes were made for 4 to 8 July 1979, 12 GMT to see how this new scheme (parabolic scheme) performs in the case of geopotential height field. In addition, the geopotential height at 700 mbar level was also analysed by FOP scheme for the same period and similarly examined.

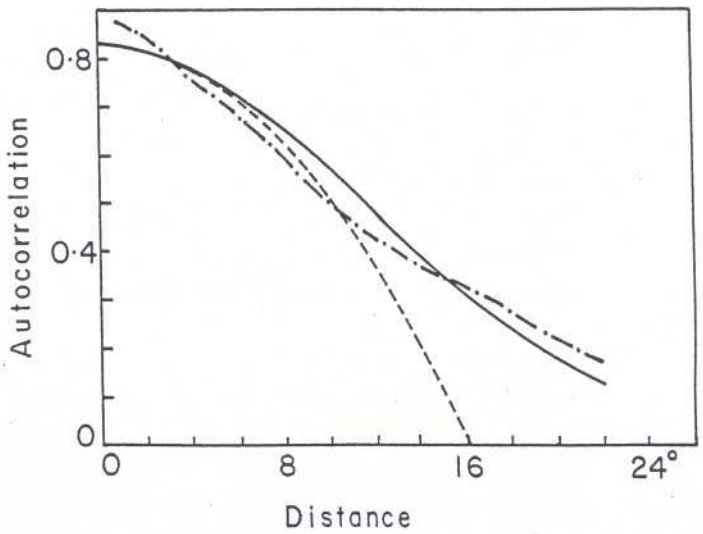

Figure 1. Observed autocorrelations (–·–·–·–·–) and autocorrelation curves for gaussian function (————) and parabola (– – – – –).

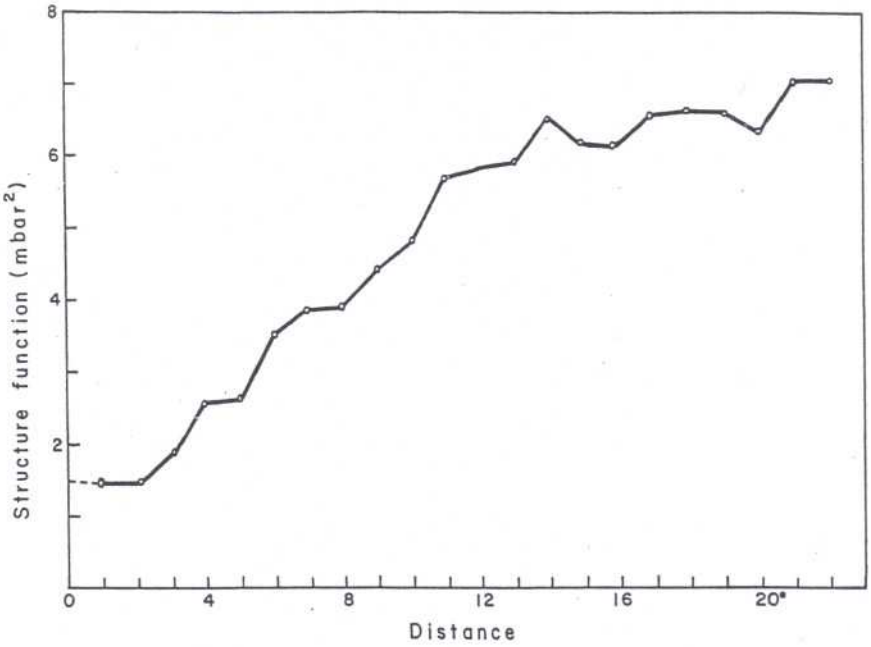

Figure 2. Structure function for MSL pressure.

Table 1. Estimate of random error (in mbar).

Variable	Extrapolated value of structure function at distance $\rho = 0$	Random error		
		$\sigma_{\varepsilon_j}^2$	σ_{ε_j}	$\hat{\lambda}$
MSL pressure	1·5	0·75	0·86	0·165

4. Discussion

The central processing unit (CPU) time for solving the necessary simultaneous equations to compute weights for 4, 6, 8, 10, 12, 14 and 16 observations was determined for gaussian scheme, parabolic and also for FOP schemes and shown in figure 3. For gaussian scheme, the CPU time increased from $0{\cdot}4 \times 10^{-2}$ to $31{\cdot}0 \times 10^{-2}$ s as the number of observations increased, whereas for parabolic and FOP schemes they remained $0{\cdot}5 \times 10^{-2}$ and $4{\cdot}0 \times 10^{-2}$ s respectively for all cases. This is because in parabolic and FOP schemes we solve only four/nine simultaneous equations irrespective of the number of observations used in the analysis for every grid point. Thus CPU time taken for parabolic scheme ($0{\cdot}5 \times 10^{-2}$ s) is an order less than for the gaussian scheme when 10 observations are used and that for the case of FOP scheme, it is slightly less than that for 10 observations in ND-560 mini supercomputer. The objective analysis of MSL pressure field of 7 July 1979 for schemes (gaussian and parabolic) is given in figures 4 and 5 for illustration. For comparison objectively analysed field of MSL pressure from FGGE (7·7·79) is reproduced here (figure 6). On examination we found that analyses using gaussian scheme (figure 4) and parabolic scheme (figure 5) were similar and that they compared well with the FGGE analysis individually (figure 6). We also found that features like low trough were brought out fairly well and the central values of lows and highs were comparable. RMS errors

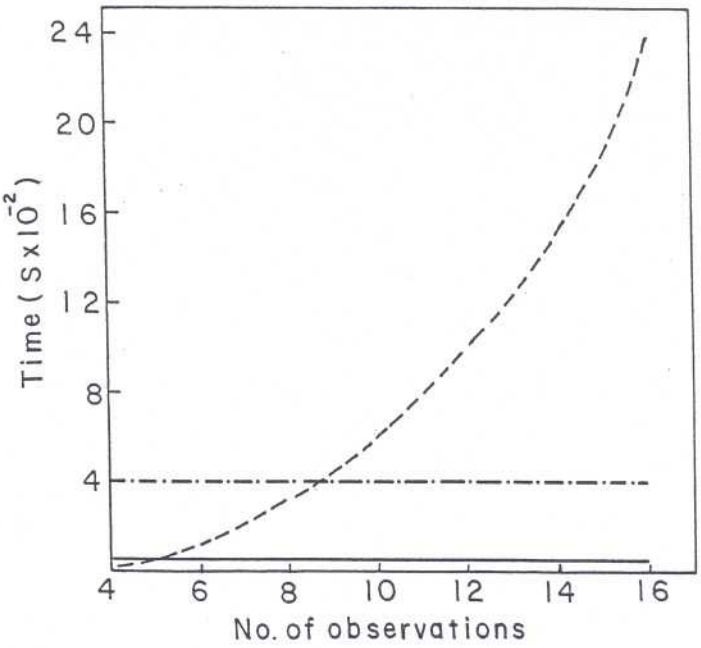

Figure 3. Timing as a function of observations for gaussian (– – – –), parabolic (————) and FOP (–·–·–·–·–) schemes.

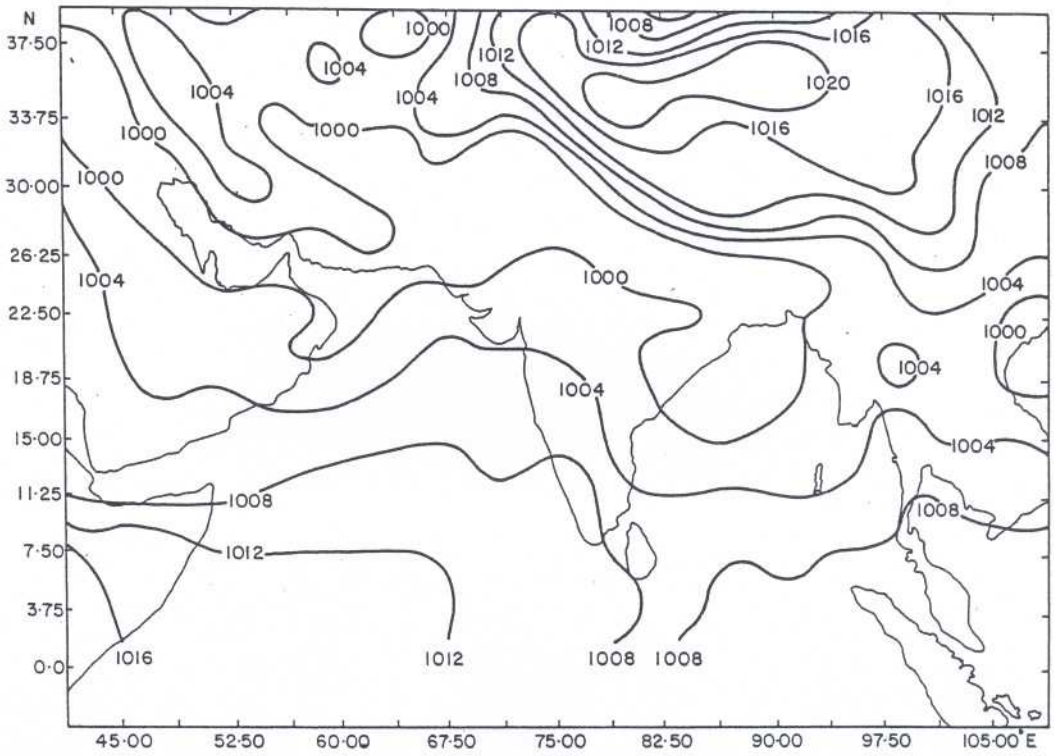

Figure 4. Objective analysis of MSL pressure of 7·7·79, for gaussian scheme.

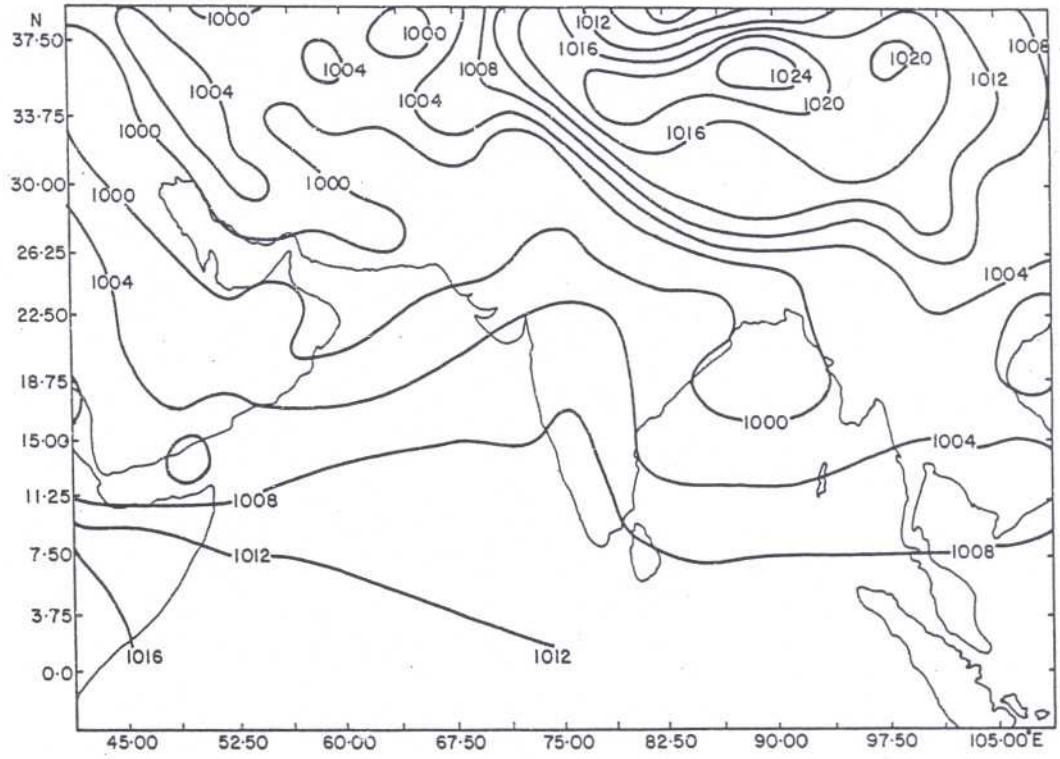

Figure 5. Same as figure 4 but for parabolic scheme.

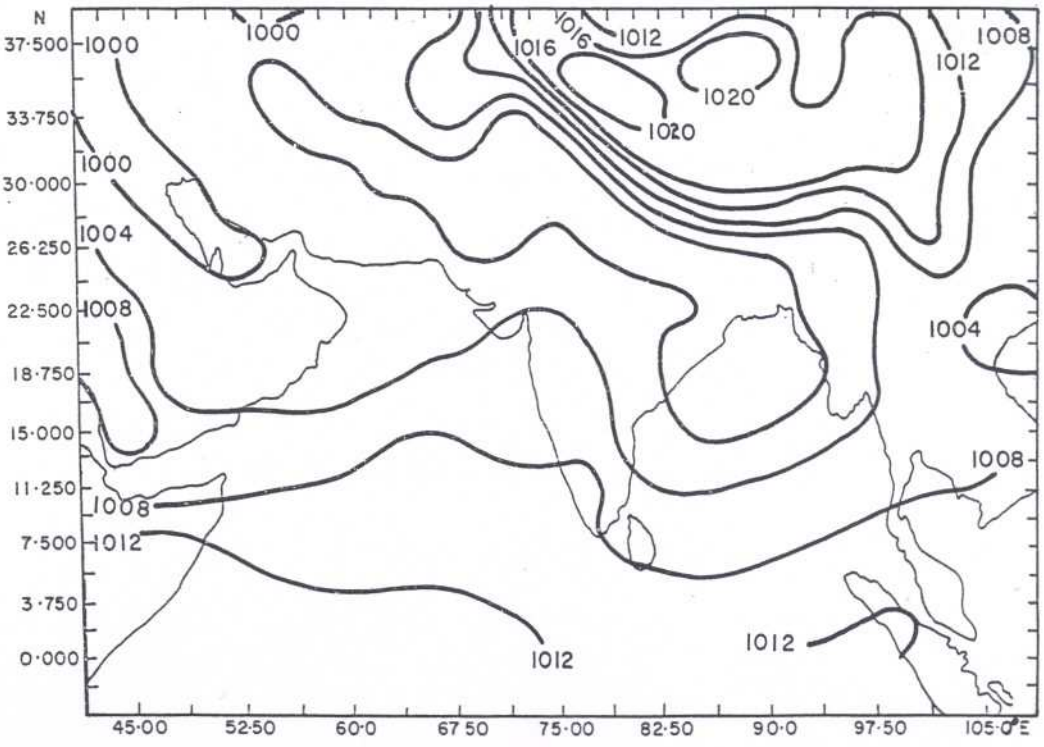

Figure 6. FGGE analysis of MSL pressure of 7·7·79.

Table 2. Root mean square errors for MSL pressure (in mbar).

Date	Compared with station observations		Compared with FGGE analyses	
	Gaussian scheme	Parabolic scheme	Gaussian scheme	Parabolic scheme
4·7·79	1·03	1·05	2·72	2·72
5·7·79	0·85	0·85	1·82	1·82
6·7·79	0·99	1·00	2·02	2·02
7·7·79	1·01	1·01	1·43	1·43
8·7·79	1·03	1·04	2·62	2·62

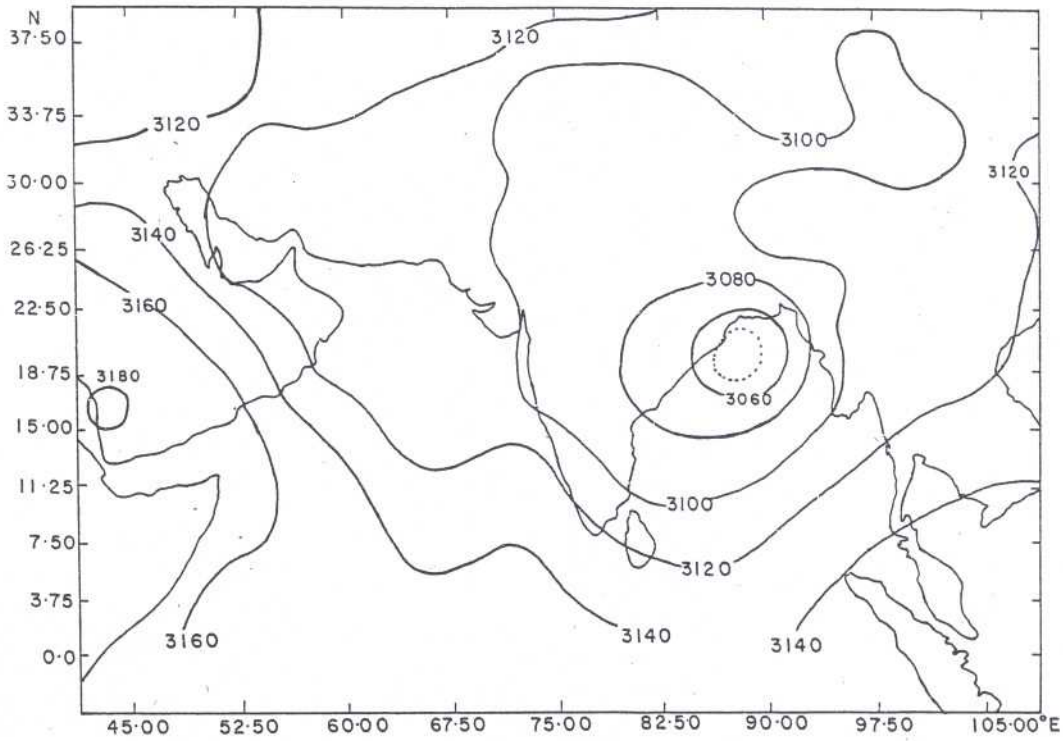

Figure 7. Same as figure 6 but for height field.

obtained are given in table 2 for MSL pressure. The RMS errors in all cases are comparatively low suggesting that the analysed fields fit well with the observations and compared well with standard analyses.

While examining the geopotential height analyses from gaussian, parabolic and FOP schemes at 700 mbar on all days, it was found that the flow patterns, the centres of the depressions/lows agreed well with each other and also with the FGGE analysis (figure 7). Figures 8, 9 and 10 show the analyses at 700 mbar for 7 July 1979 for gaussian, parabolic and FOP schemes. RMS errors are given in table 3. It could be easily seen that the RMS errors for all the three schemes are very nearly the same suggesting that the flow patterns in the three schemes are very similar. The CPU time

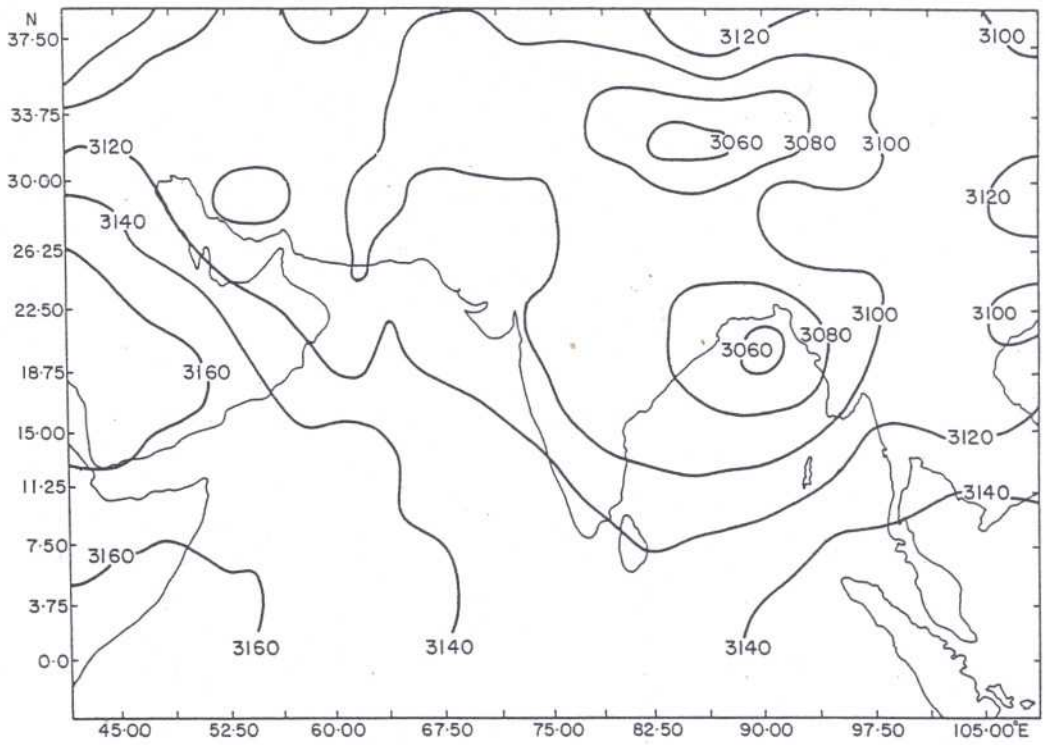

Figure 8. Height analysis of 7·7·79, 700 mbar 12 GMT for gaussian scheme.

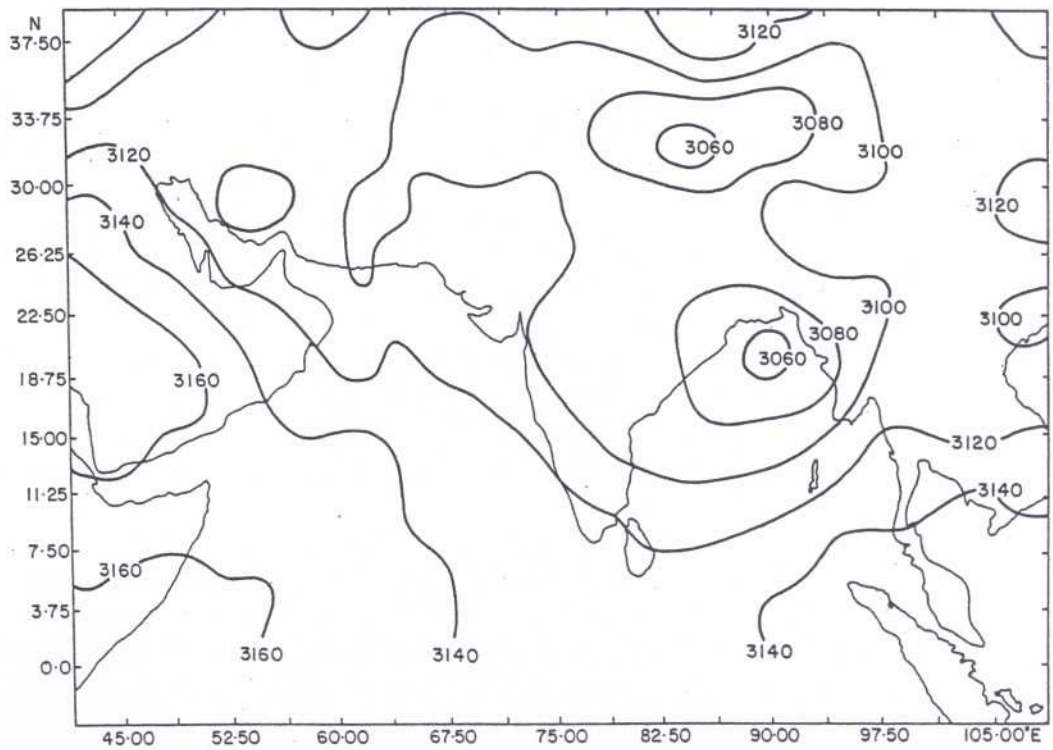

Figure 9. Same as figure 8 but for parabolic scheme.

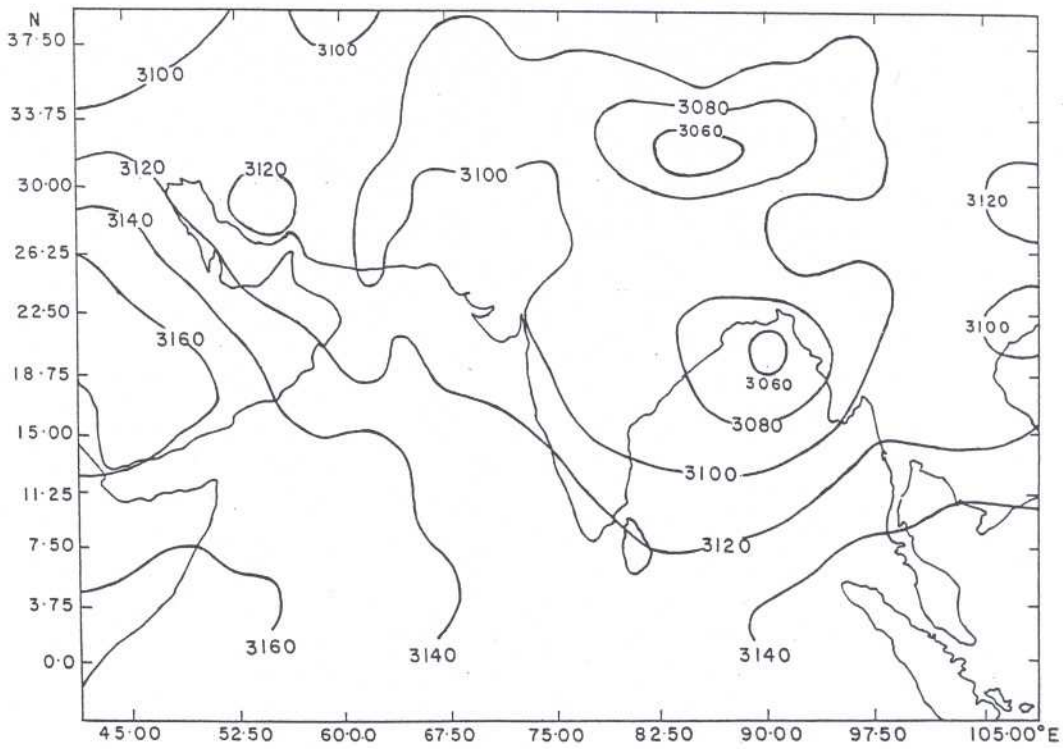

Figure 10. Same as figure 8 but for FOP scheme.

Table 3. Root mean square errors for height field (in meters).

	Compared with station observations			Compared with FGGE analyses		
Date	Guassian scheme	Parabolic scheme	FOP scheme	Gaussian scheme	Parabolic scheme	FOP scheme
4·7·79	12·99	12·60	13·43	12·36	12·24	12·31
5·7·79	12·44	12·59	13·00	14·44	14·45	14·56
6·7·79	12·53	12·27	12·63	10·64	10·69	10·44
7·7·79	14·07	14·45	14·51	10·25	10·23	10·59
8·7·79	18·57	17·61	18·63	15·27	15·15	15·12

taken for the FOP scheme is 4×10^{-2} s which is very close to the time taken by gaussian scheme for 10 observations. However, we see that the parabolic scheme which requires much less computer time is able to provide analysis similar to gaussian scheme and hence use of this scheme would be advantageous in data-rich region.

5. Conclusions

The CPU time required to determine the weights for observations in efficient optimum interpolation scheme (parabolic) is about an order less for 10 observations used for one grid point and at the same time the analyses obtained using parabolic scheme depict the flow patterns and the monsoon systems well. Further, computations of

RMS errors suggest that the parabolic scheme performs quite well compared to the gaussian scheme.

Hence, the computer time required for the parabolic scheme is minimized without sacrificing the accuracy of the analysis. The parabolic scheme is expected to be useful as the number of observations will steadily increase.

Acknowledgements

The authors thank Shri D R Sikka for his interest in this study and Drs S S Singh and P S Salvekar for their valuable comments and suggestions on the manuscript.

References

Bratseth A M 1986 Statistical interpolation by means of successive correction; *Tellus* **A38** 439–447

Franke R 1988 Statistical interpolation by iteration; *Mon. Weather Rev.* **116** 961–963

Gandin L S 1963 Objective analysis of meteorological fields; *Gidrometeorologicheskoe Izdatepstvo Leningrad*, USSR, 286

Hollingsworth A, Lorenc A C, Tracton M S, Arpe K, Cats G, Uppala S and Kallberg P 1985 The response of numerical weather prediction systems to FGGE level IIb data, Part I Analysis; *Q. J. R. Meteorol. Soc.* **111** 1–66

Jullian P R and Thiebaux H J 1975 On some properties of correlation functions used in optimum interpolation schemes; *Mon. Weather Rev.* **103** 605–616

Lorenc A C 1981 A global three-dimensional multivariate statistical interpolation scheme; *Mon. Weather Rev.* **109** 701–721

McPherson R D, Bergman K H, Kistler R E, Rasch G and Gordon D S 1979 The NMC operational global data assimilation scheme; *Mon. Weather Rev.* **107** 1445–1461

Seaman R S 1988 Some real data tests of the interpolation accuracy of Bratseth's, successive correction method; *Tellus* **A40** 173–176

Seaman R S and Hutchinson M F 1985 Comparative real data tests of some objective analysis methods by withholding observations; *Aust. Meteorol. Mag.* **33** 37–46

Shaw D B, Lonnberg P, Hollingsworth A and Unden P 1987 Data assimilation The 1984/85 revisions of the ECMWF mass and wind analysis; *Q. J. R. Meteorol. Soc.* **113** 533–566

Tanguay M and Robert A 1990 An efficient optimum interpolation analysis scheme; *Atmosphere-Ocean* **28** 365–377

Thiebaux H J 1975 Experiments with correlation representations for objective analysis; *Mon. Weather Rev.* **103** 617–627